Moho topography of the West Antarctic Rift System from inversion of aerogravity data: ramifications for geothermal heat flux and ice streaming

Michael Studinger and Robin E. Bell

Lamont-Doherty Earth Observatory of Columbia University, 61 Route 9W, Palisades, NY 10964, USA, mstuding@ldeo.columbia.edu

Summary The West Antarctic rift system, a region of thinned continental crust, dominates the lithospheric structure of the Ross Embayment in West Antarctica. It has long been hypothesized that the lithospheric structure beneath the West Antarctic Ice Sheet is a major influence on the formation, nature and dynamics of the ice sheet. The structure of the crust-mantle boundary is a fundamental geophysical parameter for understanding lithospheric processes and for geodynamic interpretation. In this paper, we use aerogravity data to derive a map of the crust/mantle boundary beneath the West Antarctic Ice Sheet and to reveal the impact of relative changes in thickness of the crust and lithosphere on surface heat flow and ice streaming.

Citation: Studinger, M., and R.E. Bell (2007), Moho topography of the West Antarctic Rift System from inversion of aerogravity data: ramifications for geothermal heat flux and ice streaming, in Antarctica: A Keystone in a Changing World – Online Proceedings of the 10th ISAES X, edited by A. K. Cooper and C. R. Raymond et al., USGS Open-File Report 2007-1047, Extended Abstract 031, 4 p.

Introduction

The West Antarctic rift system, a region of thinned continental crust, dominates the lithospheric structure of the Ross Embayment in West Antarctica (Fig. 1). This low lying region is similar in size to the Basin and Range Province of North America, and is bounded to the south and west by the Transantarctic and Whitmore Mountains and to the north and east by Marie Byrd Land. Parts of the rift are host to the West Antarctic Ice Sheet, a marine-based ice sheet prone to instability. It has long been hypothesized that the lithospheric structure beneath the West Antarctic Ice Sheet is a major influence on the formation, nature and dynamics of the ice sheet.

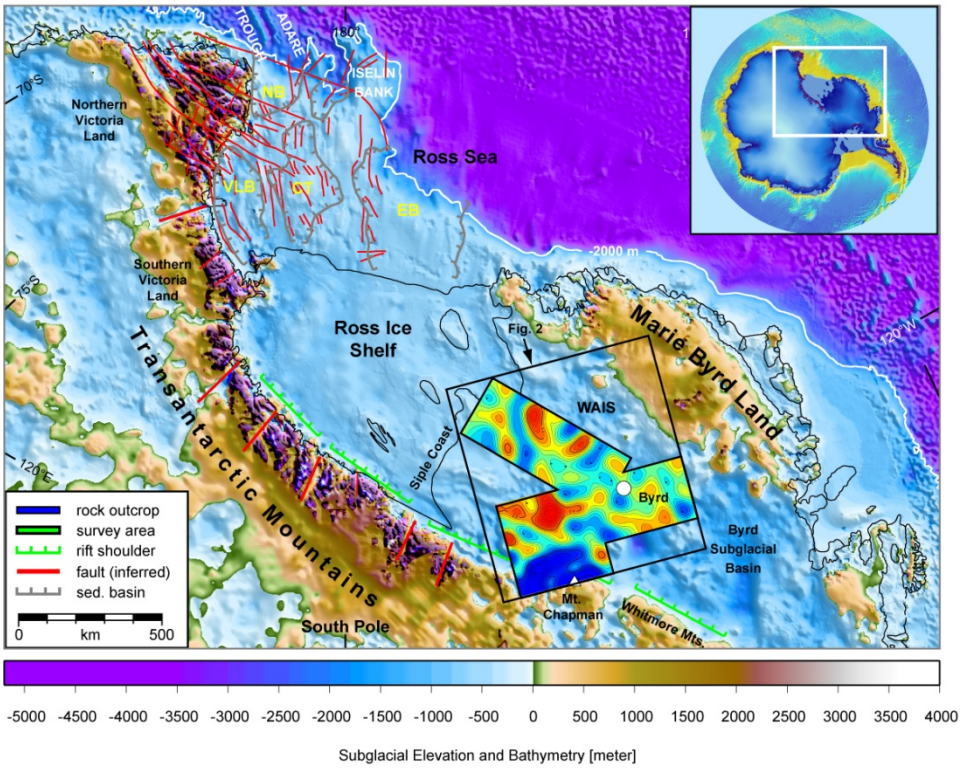

Figure 1: Location map. The West Antarctic Rift System is the entire area of intracontinental extension defined by the region under the Ross Sea, Ross Ice Shelf and the West Antarctic Ice Sheet (WAIS). The Ross Embayment comprises the Ross Sea and Ross Ice Shelf. While there is little information from the area under the Ross Ice Shelf, its western flank of the rift system is defined by the central and southern Transantarctic Mountains. The rift system's tectonic history is usually assumed to be the same as the Ross Sea. Image is using data from the BEDMAP compilation (2000) . CT, Central Trough; EB, Eastern Basin; NB, Northern Basin; TR; Terror Rift; VLB, Victoria Land Basin.

The structure of the crust-mantle boundary (i.e., the Moho discontinuity) is a fundamental geophysical parameter for understanding lithospheric processes and for geodynamic interpretation. However, crustal thickness estimates in Antarctica are limited to only a few isolated estimates beneath seismological recording sites or along targeted active seismic profiles. A major disadvantage of these seismic estimates is that structural trends in the crust/mantle boundary cannot be resolved from point measurements or along profiles. Structural trends provide important constraints on the nature and style of extension and the tectonic fabric. In this paper, we use aerogravity data to derive a map of the crust/mantle boundary beneath the West Antarctic Ice Sheet. More than 150,000 line kilometers of gravity data (*Bell et al.*, 1999) and ice thickness data (*Blankenship et al.*, 2001) have been collected by the U.S. National Science Foundation's Support Office for Aerogeophysical Research (SOAR) to compile a complete Bouguer gravity anomaly map covering 300,000 km^2 (*Studinger et al.*, 2002) (Fig. 1).

Gravity filtering

Before inverting the observed Bouguer gravity field for Moho topography the gravity effect of the crust/mantle boundary has to be isolated from shallower sources by lowpass filtering. We use a matched filter approach (*Phillips*, 1997) to design a sequence of filters. In this approach the observed radial power spectrum is matched with the model spectra of a number of equivalent source layers. First, the short wavelengths of the observed spectrum are matched with a shallow source equivalent layer model spectrum. The model spectrum is then removed from the observed power spectrum and the remaining residual spectrum is used to match the next deeper equivalent source layer. The matching of the model to the residual spectrum is continued stepwise until the entire spectrum is matched. A three layer model consisting of density layers at 3.2 and 13.7 km depth and a density half space at 27.5 km depth produces a model power spectrum that closely matches the observed spectrum. Figure 2 shows the corresponding filter functions for these three layers. The gravity effect of the crust/mantle boundary can be separated from the observed Bouguer gravity by filtering with the lowpass filter that corresponds to a density half space at z_0 = 27.5 km. The filter removes all gravity structures with wavenumbers greater than 0.2 radians/km or wavelengths shorter than 31 km.

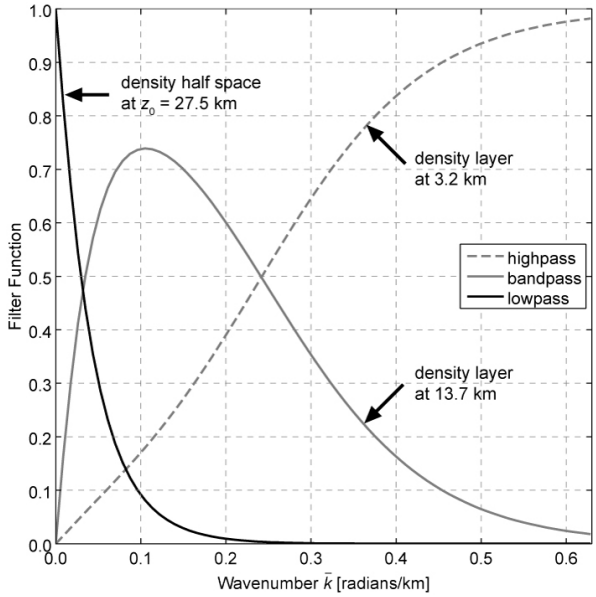

Figure 2: Filter functions derived from modeling of the observed power spectrum with 3 equivalent source layers. The lowpass filter of a density half space (solid black line) at z_0 = 27.5 km will isolate the gravity effect of the crust/mantle boundary.

Gravity inversion and comparison with seismic estimates

The lowpass filtered Bouguer gravity resulting from the three layer model was used as input for the inversion scheme. The inversion procedure used here is based on *Parker*'s algorithm for forward modeling of gravity data (1973) that has been modified by *Oldenburg* (1974) for inversion. For the inversion process, the density contrast was assumed to be 400 kg/m^3 with the mean depth z_0 to the crust/mantle boundary of 27.5 km. Convergence was usually achieved within 5 iterations. The difference between the input gravity field and the predicted gravity effect of the inverted Moho topography is 3.6 mGal which is comparable to the uncertainty in the input free-air gravity data (3 mGal) (*Bell et al.*, 1999) .

Within the survey area crustal thickness has been independently estimated from teleseismic receiver functions (*Winberry and Anandakrishnan*, 2004) and a crustal-scale seismic refraction/wide-angle-reflection experiment (*Clarke et al.*, 1997) (Fig. 3). *Winberry and Anandakrishnan* (2004) used a global average velocity model for continental crust to estimate crustal thickness with an uncertainty of ± 1 km. Four of their sites are located with the survey area. Our estimates of Moho depth compare well with the receiver function model, converted into depth below sea level, and differences are less than 2 km and generally less than 1 km (Fig. 3).

Similarly, our Moho topography agrees well with the crustal thickness model derived from refraction seismic profiling close to the Whitmore Mountains (*Clarke et al.*, 1997). The filtered gravity inversion of the Moho recovers many of the same features as the Clarke seismic refraction results although a constant offset of 2 km is evident along the profile. *Clarke et al.* (1997) noted that their crustal model can be varied by up to 2 km, with associated changes in the velocity structure, while maintaining good agreement between modeled and observed travel times. After removing an offset of 2 km from the refraction seismic estimates, the root-mean square of the difference between the seismic refraction model (transformed into depth below sea level) and our gravity inversion is 0.8 km with a maximum discrepancy of 1.3 km

(Fig. 3). The Moho topography derived from filtered gravity coincides well with two independent seismically determined Moho estimates.

Moho topography

The Moho topography derived from gravity inversion shows considerable relief between 21 and 36 km below sea level (Fig. 3). The Moho is deepest in the southeastern corner of the survey area reflecting thicker crust of the Whitmore Mountains crustal province (*Studinger et al.*, 2002). Towards the interior of the rift, the crust/mantle boundary is located at shallower depths due to thinner crust resulting from extension. Within this region the topography of the Moho varies generally between 23 and 30 km depth. Variations in Moho topography are smaller than in the Ross Sea region, where crustal thickness varies between 24 and 16 km (*Trey et al.*, 1999) consistent with the idea that crustal stretching within our survey area is significantly lower than in the Ross Sea portion of the West Antarctic rift system. The smaller amount of stretching, and by inference extension, is also consistent with the narrower topographic expression of the rift indicating that extension is fading out towards the south. The only exception is a pronounced circular region of thin crust in the southern part of the survey area where the Moho is shallowest (21 km). The shallow Moho coincides with the confluence of several ice stream tributaries and smooth and low-lying subglacial topography.

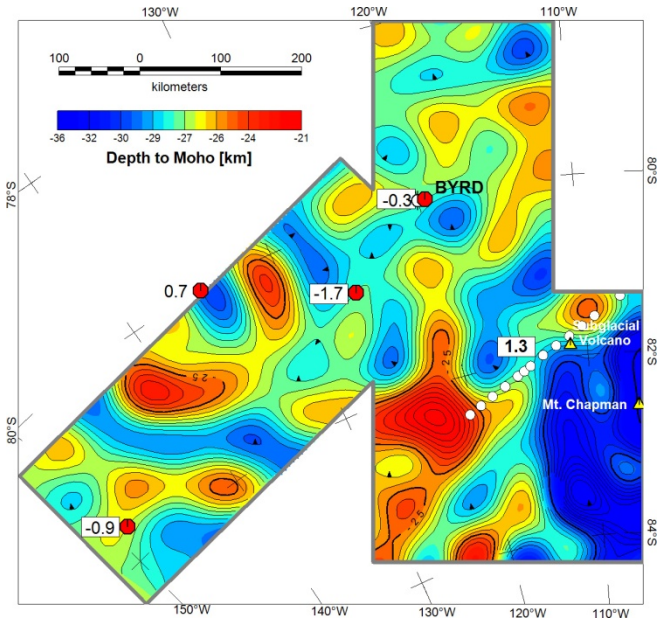

Figure 3: Depth to Moho in km below sea level estimated from gravity inversion. Contour interval is 0.5 km. Red octagons mark locations of teleseismic receiver functions estimates. Numbers mark difference between receiver function estimates and gravity inversion in km. White circles mark shot locations of a refraction seismic profile.

The map of the Moho topography shows three dominant structural trends that reflect the tectonic events that formed them. Because of the proximity of our survey area to the geographic South Pole and the resulting extreme longitudinal convergence, we have rotated all orientations into the reference longitude of the Prime Meridian (0° longitude) using *Siddoway and Siddoway*'s conversion (2006). To convert a site specific orientation to a specified reference frame (here 0° longitude) *Siddoway and Siddoway* (2006) used a transformation similar to the Antarctic Navigational Grid: S_C = MOD[(S_M + ΔL), 360] where S_C = converted orientation; S_M = site specific measured orientation; ΔL = angle in degrees longitude between the reference site and the study site (for our case ΔL = longitude of the study site); and 360 = the divisor. The conversion into a continent-wide reference frame enables direct comparison of local orientations with regional trends.

One of the trends in the Moho topography is oriented at 110°/290° (ESE/WNW) and parallel to the Transantarctic Mountains front. This trend also parallels two deep linear sedimentary basins (*Studinger et al.*, 2001) , the Whitmore Mountains province boundary, and is subparallel to the Bentley Subglacial Trench. We will refer to this ESE/WNW orientation as rift-parallel trend. The trend is also parallel to fault orientations in northern Victoria Land and the northern Ross Sea (*Salvini et al.*, 1997) . It parallels the edge of the continental shelf in the northern Ross Sea and offshore Marie Byrd Land as marked by the 2000 m isobaths.

The second trend discernible in the Moho topography is oriented perpendicular to the rift-parallel trend. This trend is oriented at 20°/200° (NNE/SSW) and we will refer to it as rift-perpendicular trend. This trend coincides with the orientation of a fault-bounded sedimentary basin identified from aerogeophysical data (*Studinger et al.*, 2001) . Along the Transantarctic Mountains front several rift-perpendicular faults exist that are often occupied by major outlet glaciers.

The third trend is oriented at 170°/350° (S/N) at an oblique angle to the rift shoulder (Fig. 1). We will refer to this trend as rift-oblique. The trend occurs near the trunk of Bindschadler Ice Stream in the south-western corner of the survey area, which is underlain by a sedimentary basin with similar trend (*Studinger et al.*, 2002) . This trend is also visible in the northern part of the survey area with elevated subglacial topography that marks the transition towards the Marie Byrd Land crustal block

Ice streaming

The relative importance of factors that control the initiation of ice streaming are still under debate but there is widespread agreement that a water saturated basal till enables fast ice stream flow (e.g., *Tulaczyk et al.*, 2000, and references

therein). The spatial pattern of ice streaming is dominated by the coupled ice-till-water system, depending on geological, glaciological, and hydrological factors. In particular, abundant, high-pressure basal water is necessary to initiate and maintain fast ice flow (e.g., *Alley et al.*, 1994). More recently, *Fahnestock et al.* (2001) and *Vogel and Tulaczyk* (2006) have shown that basal meltwater produced from localized subglacial volcanic or geothermal centers can be responsible for ice streaming. In addition to the meltwater and a weak bed, warming of the basal ice over these features will also contribute to enabling fast ice flow (*Fahnestock et al.*, 2001). Thus, geothermal heat flux is an important parameter for the formation of the water saturated lubricating till responsible for ice streaming.

Cenozoic continental rift systems are regions with significantly elevated surface heat flow (e.g., *Morgan*, 1983 and references therein) because the transient thermal perturbation to the lithosphere caused by rifting requires at least 100 my to reach long term thermal equilibrium or steady state. The geothermal heat flux measured beneath the West Antarctic Ice Sheet at Siple Dome is 69 mW/m^2 (*Engelhardt*, 2004) and is consistent with other heat flow measurements from the West Antarctic rift system (e.g., *Bücker et al.*, 2001, and references therein).

In general, the geologic contributions to continental surface heat flow can be separated into mantle heat flow and radiogenic heat flow from heat producing elements within the crust (e.g., *Roy et al.*, 1968; *Turcotte and Schubert*, 2002). The impact of relative changes in thickness of the crust and lithosphere on surface heat flow will be presented at the symposium.

Acknowledgements. Funding for this work was provided by the U.S. National Science Foundation grant ANT-03-38281 and the LDEO PGI-Doherty Fellowship. Co-editor Howard Stagg is thanked for careful reviewing and handling of the manuscript.

References

Alley, R. B., et al. (1994), A water-piracy hypothesis for the stagnation of ice stream C, Antarctica, *Annals of Glaciology*, *20*, 187-194.

Bell, R. E., et al. (1999), Airborne gravity and precise positioning for geologic applications, *J. Geophys. Res.*, *104*, 15281-15292.

Blankenship, D. D., et al. (2001), Geologic Controls on the Initiation of Rapid Basal Motion for the Ice Streams of the Southeaste rn Ross Embayment; A Geophysical Perspective Including New Airborne Radar Sounding and Laser Altimetry Results, *Antarctic Research Series, The West Antarctic Ice Sheet: Behavior and Environment*, *77*, 105-122.

Bücker, C. J., et al. (2001), Downhole Temperature, Radiogenic Heat Production, and Heat Flow from the CRP-3 Drillhole, Victoria Land Basin, Antarctica, *Terra Antartica*, *8*, 151-159.

Clarke, T. S., et al. (1997), Optimum seismic shooting and recording parameters and a preliminary crustal model for the Byrd subglacial basin, Antarctica, in *The Antarctic region; geological evolution and processes; proceedings of the VII international symposium on Antarctic earth sciences.*, edited by A. Ricci Carlo, pp. 485-493, Terra Antarctica Publication, Siena, Italy.

Engelhardt, H. (2004), Ice temperature and high geothermal flux at Siple Dome, West Antarctica, from borehole measurements, *J. Glaciol.*, *50*, 251-256.

Fahnestock, M., et al. (2001), High geothermal heat flow, basal melt, and the origin of rapid ice flow in central Greenland, *Science*, *294*, 2338-2342.

Lythe, M. B., et al. (2000), BEDMAP - bed topography of the Antarctic, British Antarctic Survey, Cambridge.

Morgan, P. (1983), Constraints on rift thermal processes from heat flow and uplift, *Tectonophysics*, *94*, 277-298.

Oldenburg, D. W. (1974), The inversion and interpretation of gravity anomalies, *Geophysics*, *39*, 526-536.

Parker, R. L. (1973), Rapid Calculation of Potential Anomalies, *Geophys. J. R. Astron. Soc.*, *31*, 447-455.

Phillips, J. D. (1997), *Potential-field geophysical software for the PC, version 2.2*, 34 pp., U. S. Geological Survey, Reston, VA, United States.

Roy, R. F., et al. (1968), Heat Flow in United States, *Journal of Geophysical Research*, *73*, 5207-&.

Salvini, F., et al. (1997), Cenozoic geodynamics of the Ross Sea region, Antarctica: Crustal extension, intraplate strike-slip faulting, and tectonic inheritance, *J. Geophys. Res.*, *102*, 24669-24624,24696.

Siddoway, C., and M. F. Siddoway (2006), Addressing the longitudinal reference problem in Antarctica: a method for regional comparison of structural data using modular arithmetic, *Terra Antartica Reports*, *12*, 119-132.

Studinger, M., et al. (2001), Subglacial sediments: A regional geological template for ice flow in West Antarctica, *Geophys. Res. Lett.*, *28*, 3493-3496.

Studinger, M., et al. (2002), Mesocoic and Cenozoic extensional tectonics of the West Antarctic, in *Antarctica at the close of a millennium*, edited by J. A. Gamble, et al., pp. 563-569, The Royal Society of New Zealand, Wellington, New Zealand.

Trey, H., et al. (1999), Transect across the West Antarctic rift system in the Ross Sea, Antarctica, *Tectonophysics*, *301*, 61-74.

Tulaczyk, S., et al. (2000), Basal mechanics of Ice Stream B, West Antarctica 2. Undrained plastic bed model, *J. Geophys. Res.-Solid Earth*, *105*, 483-494.

Turcotte, D. L., and G. Schubert (2002), *Geodynamics*, 456 pp., Cambridge University Press, Cambridge, United Kingdom.

Vogel, S. W., and S. Tulaczyk (2006), Ice-dynamical constraints on the existence and impact of subglacial volcanism on West Antarctic ice sheet stability, *Geophys. Res. Lett.*, *33*.

Winberry, J. P., and S. Anandakrishnan (2004), Crustal structure of the West Antarctic rift system and Marie Byrd Land hotspot, *Geology*, *32*, 977-980.